Int. J. Electrochem. Sci., 6 **(2011)** 506 - 519

International Journal of
ELECTROCHEMICAL
SCIENCE
www.electrochemsci.org

Electrochemical Study of a Simulated Spent Pickling Solution

M. García-Gabaldón[*], *J. Carrillo-Abad, E. Ortega-Navarro, V. Pérez-Herranz*

IEC Group. Departamento de Ingeniería Química y Nuclear. Universidad Politécnica de Valencia. P.O. Box 22012, E-46071 Valencia. Spain
[*]E-mail: mongarga@iqn.upv.es

Received: 12 January 2011 / *Accepted:* 20 January 2011 / *Published:* 1 February 2011

The electrochemical behaviour of the main components of the rinsing pickling solutions of the hot dip galvanizing industry, Zn^{2+} and Fe^{2+} in HCl, was studied by cyclic voltammetry. The effect of different variables (such as the scan rate, the inversion potential, the addition of zinc, stirring of the solution and the presence of iron) on the current-potential curves was studied. The electrochemical reduction of zinc proceeded by a typical nucleation process. Decreasing the HCl concentration enhanced the zinc UPD process because of the less influence of the hydrogen evolution reaction (HER), and a prepeak corresponding to the zinc UPD process was observed previously to the zinc OPD step. The effect of the scan rate on the OPD peak was studied and showed that the Zn^{2+} reduction was an irreversible process which was not only controlled by diffusion but also charge transfer kinetics. The diffusion coefficient of zinc was calculated (1.66×10^{-9} m^2s^{-1}). In view of iron deposition, it was confirmed that the pH is an essentially important factor and at low pH values was virtually impossible to deposit iron. The electrochemical study of mixtures containing both zinc and iron showed that the presence of zinc produced an inhibition of the iron deposition process which was confirmed by the observation of the deposits. The SEM images revealed only the presence of zinc grains. However, if the ratio Fe(II)/Zn(II) was higher, the voltammograms main features were more similar to those obtained for pure iron solutions.

Keywords: Pickling baths**,** zinc, iron, electrochemical deposition, cyclic voltammetry, hot dip galvanizing

1. INTRODUCTION

Every year the political economy suffers under the loss of money caused by atmospheric attack of steel construction parts. A simple and effective way for corrosion protection is the coating of the unalloyed steel with a thin layer of metallic zinc. The zinc coating is widely employed on steel to control the corrosion process [1]. Most of the treated material is coated with zinc by hot dip

galvanizing. This process consists of the following steps: alkaline or acidic degreasing, rinsing with water, pickling with dilute hydrochloric or sulphuric acid, rinsing with water, fluxing in aqueous $ZnCl_2/NH_4Cl$ baths, drying and dipping into molten zinc at temperatures of about 450ºC for a defined period [2].

In the case of the hydrochloric acid pickling at hot dip galvanizing plants, HCl is used to remove rust from the steel and this process results in large volumes of iron and zinc contaminated low acid wastes across the industry. As pickling proceeds, HCl reacts with iron and iron oxides to form ferrous chloride in solution.

This continues until the acid concentration falls to give unacceptable pickling times. The remaining acid is then usually used for stripping zinc from rejected galvanizing work until the acid is deemed spent. Zinc may also enter the pickling line via hooks, jigs, etc., that are used to suspend the work during dipping. Spent pickling acid is, therefore, a solution containing various concentrations of HCl, $FeCl_2$ and $ZnCl_2$ [3] and its composition varies greatly depending on how long it has been used for pickling. Spent pickling liquors from treating common steels in metal working industries mainly contain 80-150 g/l $FeCl_2$, 5-150 g/l $ZnCl_2$ and 10-80 g/l HCl [2].

The presence of these metallic ions decreases the efficiency of the process and the acid needs to be replaced by clean acid when a certain concentration of iron is reached in the bath. The spent bath thus becomes a residue with a high pollution potential, the management of which supposes important economic and environmental costs [4].

Eliminating zinc from the solution by its cathodic electrodeposition should allow recycle of the residual solution, although small amounts of the metal is still contained. On the other hand, electrolytic recovery of zinc is one of the oldest industrial processes, whose importance lies in the great worldwide demand for this metal that currently reaches an overall production of 9 million tonnes per year [5].

In this way, the selective electrochemical separation of the metals present in a solution depends on their relative deposition potentials, so that if the deposition potentials are quite different then it will be possible to separate the metals.

However, a previous study of the chemical and electrochemical behaviour of the metal ions must be done in order to examine the kinetic characteristics for the desired reactions and to take account of complexation of the cations and the irreversible nature of the electrodeposition processes [6].

The present work deals with the investigation of the electrochemical behaviour of the spent acid pickling baths. Cyclic voltammetry was used to characterize the kinetics of the electrodeposition of zinc in chloride-based acidic media, and the effect of iron on zinc electrodeposition. This information will be helpful for a further study about the feasibility of the recovery of zinc from the wasted pickling solutions or from the rinsing baths using an electrochemical reactor. Due to the great complexity of the acid pickling solutions and to the presence of different additives, solutions of Zn^{2+} and Fe^{2+} in HCl, simulating the composition of the real baths, were firstly prepared and studied in the present paper as a previous step to the investigation of the wasted pickling solutions and the rinsing baths.

2. EXPERIMENTAL SECTION

All solutions were prepared using analytical grade reagents. Electrolytes containing $ZnCl_2$ in HCl with and without $FeCl_2 \cdot 4H_2O$ were used in a concentration range similar to that present in the rinsing pickling baths. All solutions were prepared with distilled water.

The effect of different variables on zinc deposition, such as the scan rate, the inversion potential, the addition of zinc, stirring of the solution and the presence of iron, were investigated by cyclic voltammetry using a conventional three-electrode cell. The working electrode was a platinum disc of surface area 0.078 cm^2 enclosed in Teflon. Prior to each experiment, the Pt surface was mechanically polished with emery paper down to 4000 grit. An Ag/AgCl saturated KCl electrode was used as the reference electrode and a platinum electrode was used as the counter electrode. All potentials reported here are expressed with respect to the Ag/AgCl electrode. Before each electrochemical experiment, the solution was deoxygenated for 10 minutes with ultrapure nitrogen. This inert atmosphere was maintained during the whole measurement. The electrochemical experiments were controlled using an Autolab PGSTAT20 potentiostat/galvanostat. The scan rate was varied from 5 to 100 mVs^{-1}. The initial potential was the open circuit potential, and the polarisation was first in the negative direction. All experiments were carried out at room temperature.

Zinc was deposited under potentiosotatic conditions (-0.5V and -1.4V) during 2 hours onto the Pt substrate. The structure, morphology and composition of the zinc coatings were examined by means of a JEOL JSM-3600 scanning electron microscope.

3. RESULTS AND DISCUSSION

3.1. Studies on Zn^{2+} solutions

A typical cyclic voltammogram of platinum recorded in 0.055M $ZnCl_2$, between the open circuit potential (0.43V) and -2V is shown in Fig. 1 (red line). The voltammogram main features are the sharp cathodic peak C1, and the corresponding anodic stripping peak A1. A shoulder C2 is observed between -0.3 and -1.25V. In what concerns to peak C1, centred at -1.5V, it corresponds to the zinc bulk deposition. In this potential region the hydrogen evolution also occurs, as detected by direct observation, and is reflected by the current oscillations present in Fig. 1. Upon the sweep reversal, two current crossovers appear indicating the formation of stable growth centres at the substrate surface [7]. The potential at which the more cathodic crossover occurs is known as the nucleation potential and the second crossover is known as the crossover potential. The presence of these two crossovers is characteristic of processes involving nucleation [7-9]. The anodic peak A1 centred at -0.6V is attributed to the oxidation of metallic zinc to Zn^{2+}. Beyond peak A1 the current approaches to zero, indicating that the majority of the deposited zinc has been removed from the substrate surface.

A voltammogram in the absence of zinc ions is also presented in Fig. 1 (green line). The comparison of the voltammograms obtained in the presence and absence of zinc ions suggests that shoulder C2 is due to hydrogen evolution since this reaction occurs significantly at these potentials

when the zinc ions are absent. Others authors have found similar results [10-12]. On the other hand, the presence of zinc in solution leads to a decrease in the hydrogen evolution rate. On the positive scan, no anodic peak related to C2 is observed, indicating that the hydrogen reduction process is irreversible.

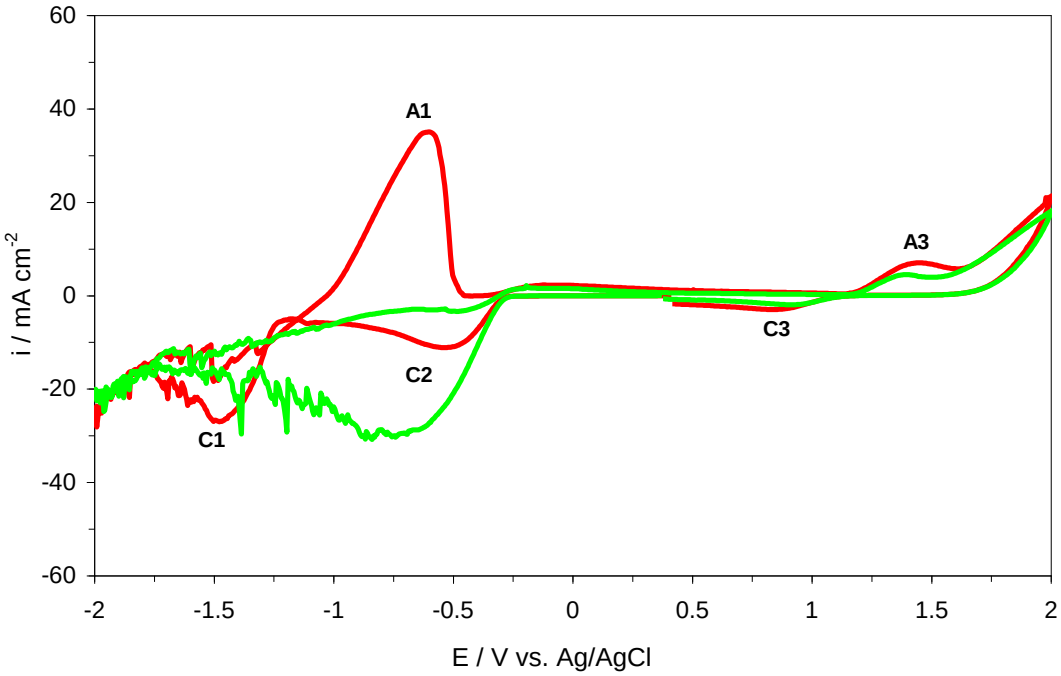

Figure 1. Cyclic voltammogram obtained for a platinum electrode in a 0.055M $ZnCl_2$ in 0.05M HCl electrolyte (red line) and in 0.05M HCl (green line). Scan rate 60 mVs^{-1}.

Both curves presented in Fig. 1 present common peaks (C3 and A3). The presence of the cathodic peak referred as C3 at 0.9V is attributed to the reduction of the chlorine bubbles adhered to the electrode. The reduction of chlorine gas is a well known phenomenon at platinised platinum electrodes [13, 14]. On the other hand, peak A3 placed at about 1.5V refers to the chloride to chlorine oxidation.

Fig. 2 illustrates the effect of the HCl concentration on the shape of the voltammograms in the 0.055M $ZnCl_2$ electrolyte. At 0M HCl (curve a)), no hydrogen evolution is observed, and a peak at -1.4V (C1) is noticed, which corresponds to zinc bulk deposition.

With the increase of the HCl concentration, hydrogen bubbles are visible with the naked eye from a potential value of -0.45V, due to the catalytic activity of platinum, and this is the potential region where the course of the voltammogram changes. With the decrease of the electrolyte pH, the rate of the overall cathode reaction increases, as observed by the increase of peak C2 related to the hydrogen evolution reaction. Moreover, as the HCl concentration is higher, peak C1 is shifted towards more cathodic potential values and an increase in area of the anodic peak related to zinc dissolution (A1) is also observed.

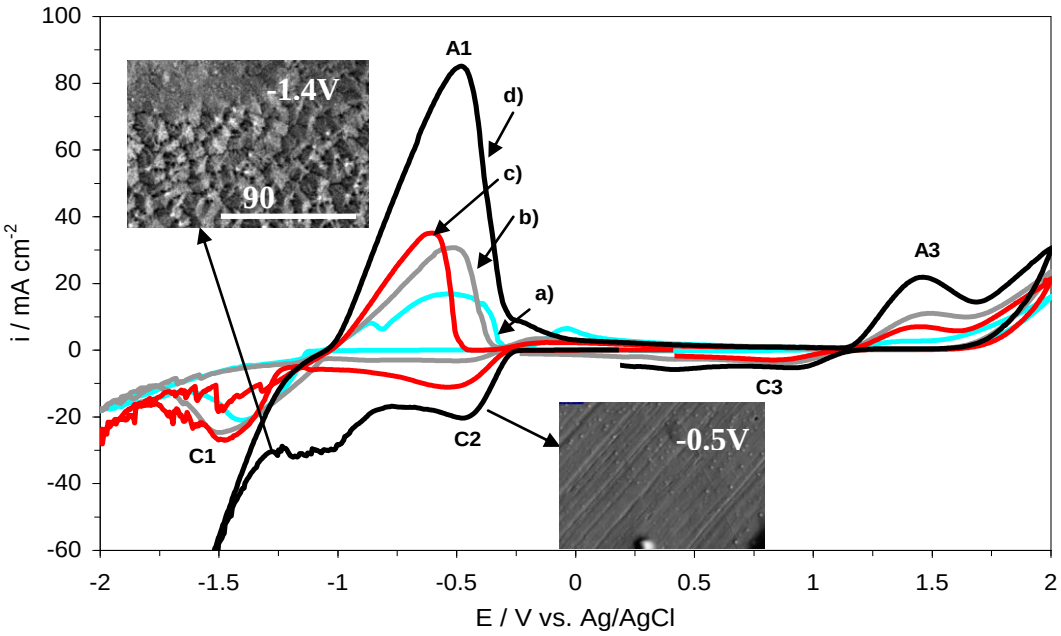

Figure 2. Cyclic voltammogram of a 0.055M $ZnCl_2$ electrolyte as a function of the HCl concentration: a) 0M HCl; b) 0.01M HCl; c) 0.05M HCl; d) 0.1M HCl. Insets correspond to the SEM images of the zinc deposits obtained at -0.5 and -1.4V in presence of a 0.055M $ZnCl_2$ in 0.1M HCl electrolyte.

Zinc deposits obtained at -0.5V (peak C2) and -1.4V (peak C1) during 2 hours and under the experimental conditions presented in Fig. 2d) were analysed by SEM and are shown in the insets of Fig. 2. The zinc percentage in the deposit obtained at -0.5V is negligible, since the HCl concentration in solution is quite high and this potential value belongs to the hydrogen evolution range. On the contrary, when the potentiostatic experiments are performed at -1.4V, the typical morphology of a zinc deposit [15] is obtained.

Fig. 3 shows the voltammograms obtained in a 0.055M $ZnCl_2$ in 0.05M HCl electrolyte at different switching potentials (E_λ). As expected, changes on the inversion potential to less negative values lead to a decrease of the anodic peak size, accompanied by a negative shift of the peak potential due to an easier dissolution of the deposit. If the switching potential E_λ is less cathodic than -1V, no anodic peak is observed, since under these potential values the contribution of zinc reduction to the overall cathodic current is very low.

Fig. 4 presents the effect of zinc concentration on the cyclic voltammograms obtained at 0.05M HCl and a scan rate of $60mVs^{-1}$. An increase in the zinc concentration leads to a rise in the rate of deposition of this species which is reflected by an increment of the cathodic peak (C1) and its corresponding counterpeak (A1). On the other hand, as the zinc concentration increases, peak C1 shifts towards more cathodic values, and consequently, peak A1 moves to less cathodic potential values. The current oscillations observed reflect the strong influence of the hydrogen evolution under static conditions.

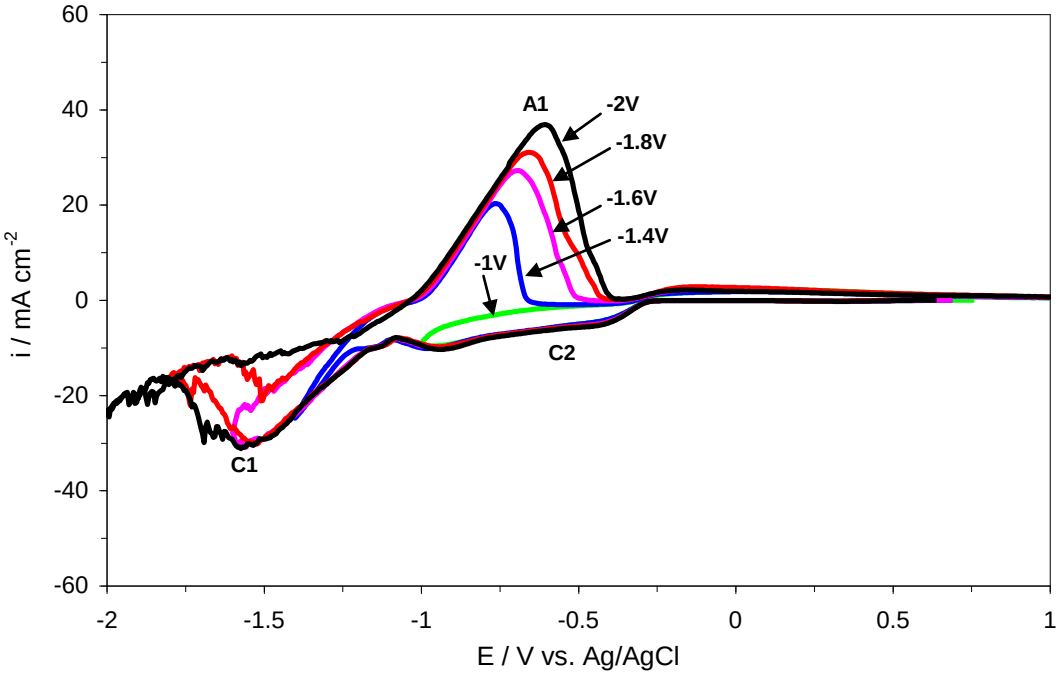

Figure 3. Cyclic voltammograms obtained for a platinum electrode in a 0.055M $ZnCl_2$ in 0.05M HCl electrolyte as a function of the inversion potentials. Scan rate 60 mVs^{-1}.

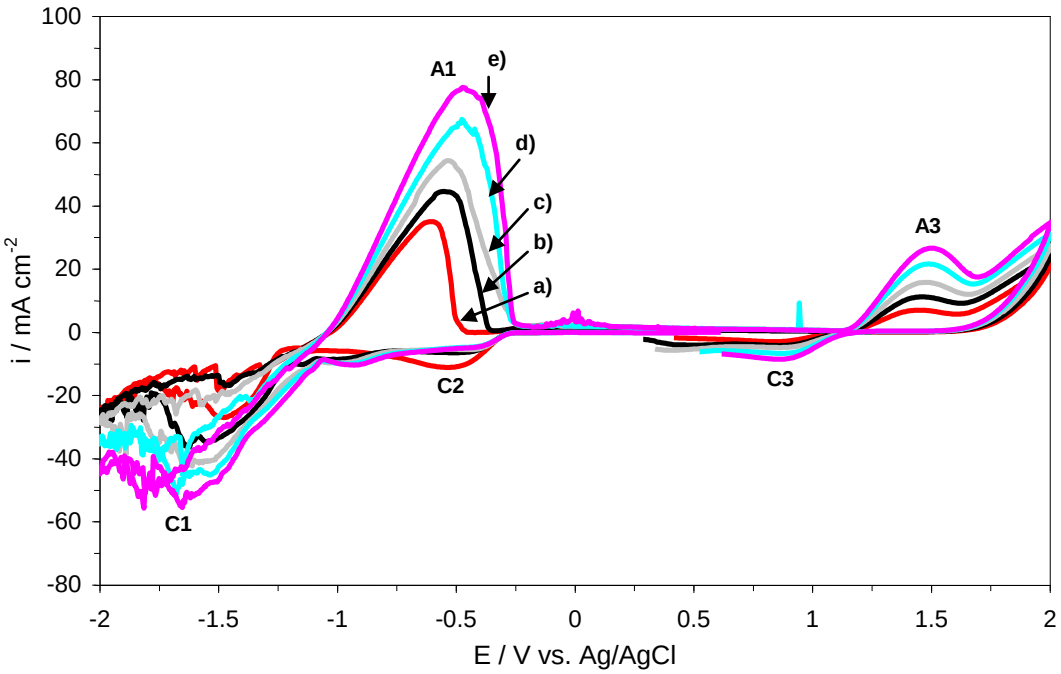

Figure 4. Cyclic voltammograms obtained in 0.05M HCl at different zinc concentrations: a) 0.055M $ZnCl_2$; b) 0.073M $ZnCl_2$; c) 0.09M $ZnCl_2$; d) 0.106 $ZnCl_2$; e) 0.12M $ZnCl_2$. Scan rate 60 mVs^{-1}

Fig. 5 illustrates the effect of the stirring velocity on the zinc deposition. When the supporting electrolyte is absent, Fig. 5a), a rise in the rotation rate leads to an increase in peaks C1 and A1, and a

displacement to more and less cathodic potential values, respectively. This behaviour is characteristic of electrochemical processes under mass transfer control, which have been demonstrated in previous studies [16]. When the HCl concentration in solution is 0.05M, Fig. 5b), peak C2 related to the hydrogen evolution reaction (HER) remains constant as expected for an irreversible process under charge transfer control. Moreover, peak C1 associated with bulk zinc deposition shifts towards less negative potential values as the rotation rate is higher. Therefore, an increase of the rotation speed leads to an increment of the cathodic peak C1, proving that bulk zinc deposition process is dominated by the mass transfer phenomenon [17, 18].

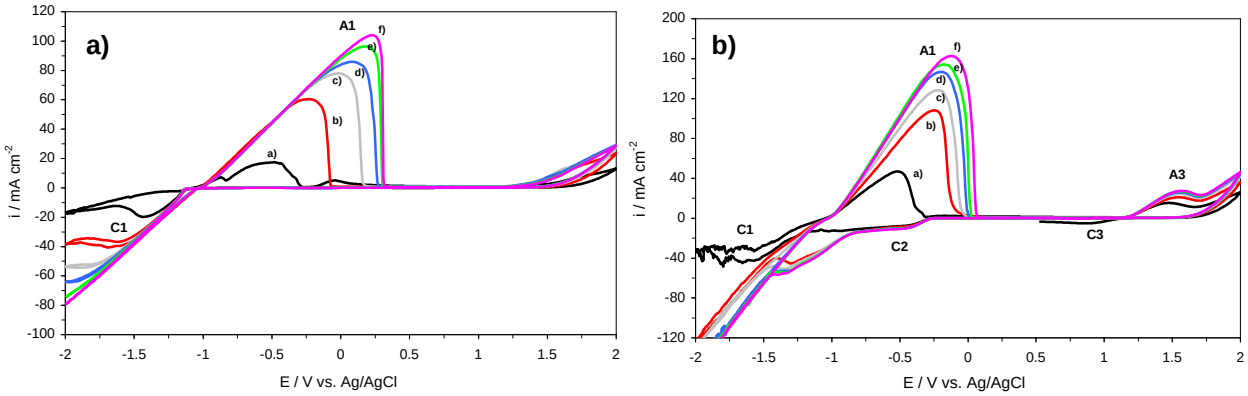

Figure 5. a): Cyclic voltammograms of a 0.055M $ZnCl_2$ solution at different rotation rates: a) 0rpm; b) 500rpm; c) 1000rpm; d) 1500rpm; e) 2000rpm; f) 2500rpm. **b)**: Cyclic voltammograms of a 0.055M $ZnCl_2$ in 0.05M HCl solution at different rotation rates: a) 0rpm; b) 500rpm; c) 1000rpm; d) 1500rpm; e) 2000rpm; f) 2500rpm.

Fig. 6 shows a set of cyclic voltammograms obtained in the 0.055M $ZnCl_2$ solution as a function of the scan rate (ν). During the direct scan it is possible to note the formation of two peaks C1 and C'1 placed at potential values of -1.25 and -0.2V, respectively. Upon reversing the scan, their respective anodic counterpeaks at -0.8V (A1) and -0.1V (A'1) are observed. The potential of peak C'1 (-0.2V) is located at more positive potential values than the equilibrium potential of the zinc system (-0.99V vs. Ag/AgCl), which is characteristic of an underpotential deposition process (UPD). In this potential region, it may be possible to get zinc monolayers accordingly with the characteristics of the deposits obtained within the underpotential condition [19]. Peak C1 observed at about -1.25V corresponds to a tridimensional nucleation and growth of the zinc deposits in the overpotential deposition region (OPD zone). Under these conditions, zinc deposits are massive and random as shown in the inset of Fig. 2 that corresponds to a zinc deposit obtained at -1.4V. It is important to mention that the magnitude of the integrated charge under the UPD region is found to be 261$\mu C \cdot cm^{-2}$ and the theoretical charge for a zinc monolayer on Pt [20] corresponds to 294 $\mu C \cdot cm^{-2}$. This evidence also supports the existence of a zinc UPD process onto the platinum electrode. The UPD of zinc on platinum has been studied extensively over recent decades, since it can give wide changes in the electronic and electrocatalytic properties of the metal surface [18, 20-25].

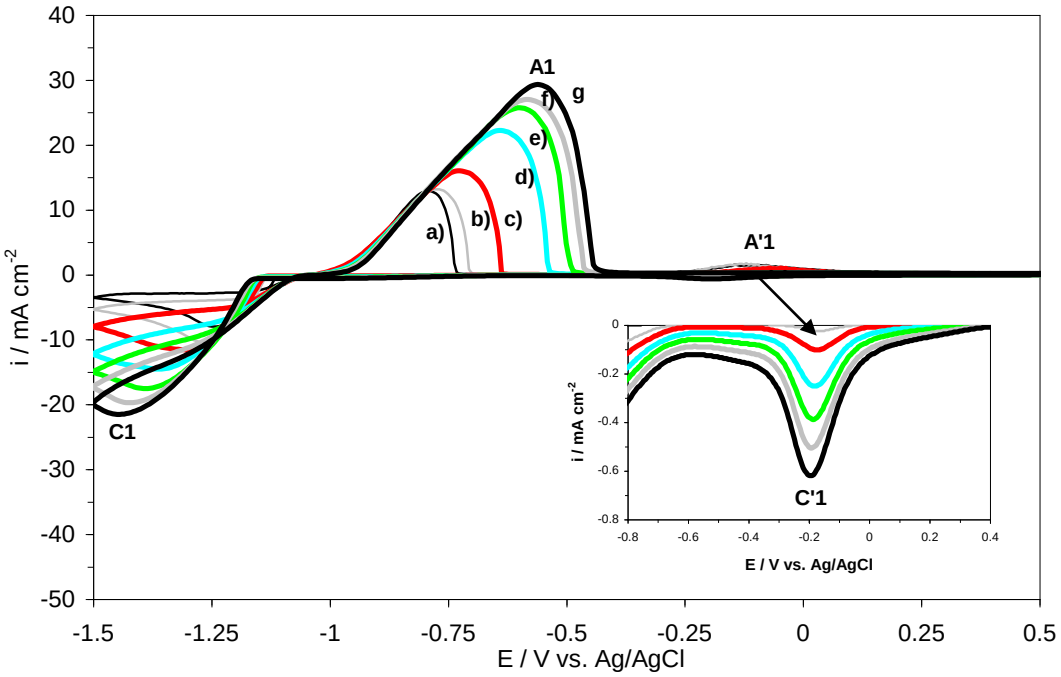

Figure 6. Cyclic voltammograms of a 0.055M $ZnCl_2$ solution at different scan rates: a) 5 mVs^{-1}; b) 10 mVs^{-1}; c) 20 mVs^{-1}; d) 40 mVs^{-1}; e) 60 mVs^{-1}; f) 80 mVs^{-1}; g) 100 mVs^{-1}.

According to some authors, the potential shift for Zn UPD on platinum, i.e. the potential difference between bulk zinc deposition (OPD) and UPD ranges from 1.04 to 1.19V [22], which is in accordance with the data presented in Fig. 6. The process of zinc UPD occurs simultaneously with hydrogen adsorption, thus the integration of the charge for the zinc UPD layer is difficult and it is not clear to what extent zinc UPD forms preferentially with respect to hydrogen adsorption. This is the reason why when the HCl is present in solution, the peak corresponding to the zinc UPD (C'1) is masked by the HER (Fig. 1).

In order to determine the type of control limiting the UPD and the OPD processes, the current associated with both peaks C1 and C'1 (I_p) is plotted as a function of $\nu^{1/2}$ in Fig. 7a) and 8a), respectively. The variation is linear in both cases but the line does not pass through the origin in the case of peak C1. The linearity is expected for a reduction process that occurs under diffusion control, however, the intercept higher than zero in the case of peak C1 indicates that an additional process other than diffusion occurs [16] during the process of zinc OPD.

Figures 7b) and 8b) present the dependence of both peak potentials (E_p) on the logarithm of the scan rate. Note that in Fig. 8b), the potential related to peak C'1 does not change appreciably with ν. Last behaviour is typical of the reversible underpotential deposition process. In what concerns to the peak potential of C1, it does change appreciably with ν as shown in Fig. 7b). In this latter case, the difference in the value of $|E_p - E_{p/2}|$ is much larger than the value required [26-28] for a reversible process (24.7 mV at 373K) [29] indicating that the bulk reduction of Zn^{2+} at a Pt electrode is not only controlled by diffusion but also charge transfer kinetics.

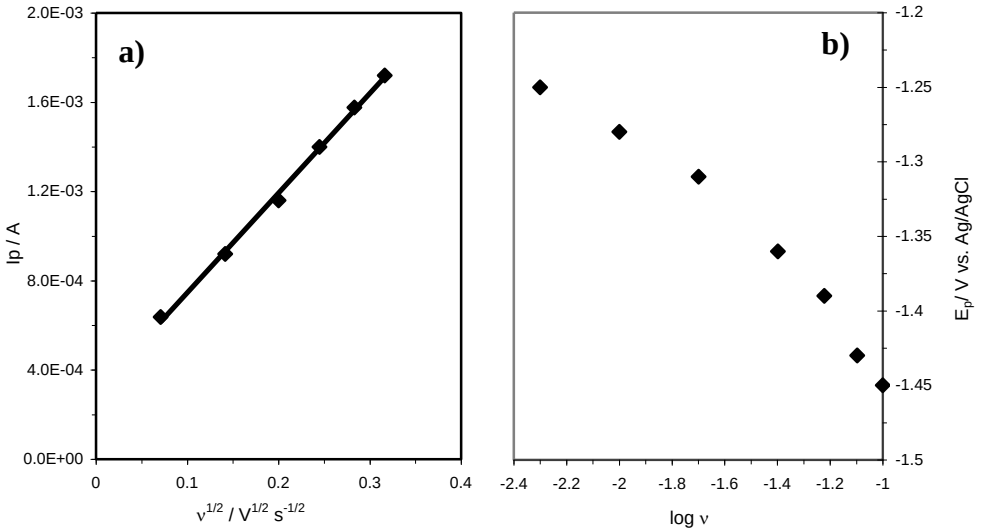

Figure 7. a): Plot of the current of peak C1 against the square root of scan rate. **b):** Plot of the potential of peak C1 versus the logarithm of the scan rate.

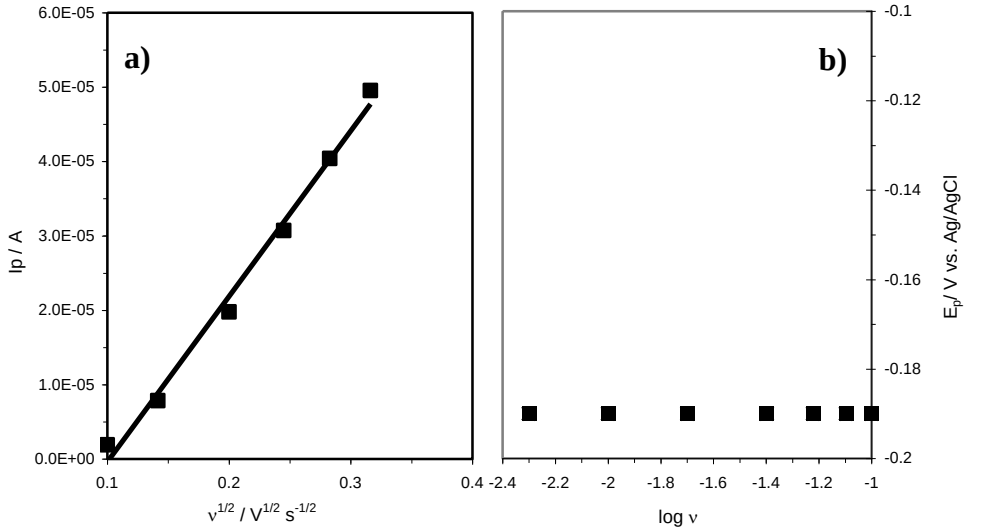

Figure 8. a): Plot of the current of peak C'1 against the square root of scan rate. **b)**: Plot of the potential of peak C'1 versus the logarithm of the scan rate.

The potential of peak C1 shifts negatively by 170 mV per 10-fold increase in the scan rate (Fig. 7b)), which is characteristic of an irreversible electrode process [26], since in these processes E_p shifts $-30/\alpha \cdot n_\alpha$ mV for each decade increase in ν [30]. The value of $\alpha \cdot n_\alpha$ can be determined [26] from the shift in E_p per 10-fold increase in scan rate by the following equation:

$$\Delta E_p = \frac{1.15RT}{\alpha \cdot n_\alpha F} \qquad (1)$$

where α is the charge transfer coefficient and represents a measure of symmetry barrier in a non-reversible electrode process, n_α is the number of electrons involved in the rate determining step, F the Faraday constant and T is the absolute temperature in K. The value of $\alpha \cdot n_\alpha$ was found to be 0.174 for the experimental data presented in Fig. 7b).

A relation between the cathodic peak current (I_p) and the scan rate (ν) for an irreversible process leading to the formation of insoluble product is given by the following equation [26, 27]:

$$I_p = 0.496nFCAD^{1/2}\left(\frac{(\alpha \cdot n_\alpha)F\nu}{RT}\right)^{1/2} \quad (2)$$

where n is the number of electrons transferred, A is the electrode area in cm^2 (0.08 cm^2), D is the diffusion coefficient of the species being reduced in cm^2s^{-1}, C is the zinc concentration in the bulk solution in mol/cm^3 and ν is the scan rate in V/s. From the slope of the straight line corresponding to the linear fit of the experimental data presented in Fig. 7a) and using equation (2), the diffusion coefficient of the zinc OPD process is determined, which gives a value of $1.66 \cdot 10^{-9}$ m^2 s^{-1}. The latter value is very similar to other reported values [20, 31].

3.2. Studies of mixtures containing Zn^{2+} and Fe^{2+}

Previously to the study of mixtures containing zinc and iron in a composition similar to that present in the real pickling baths, it is necessary to perform an electrochemical study of solutions containing Fe^{2+} in HCl. Fig. 9 shows a set of cyclic voltammograms corresponding to iron deposition for different HCl concentrations. In view of iron deposition, it is confirmed that the pH is an essentially important factor as this deposition is accompanied by the simultaneous evolution of hydrogen from the very beginning of the metal deposition [32]. When the supporting electrolyte is absent, the predominant cathode reaction is the reduction of Fe^{2+} to metallic iron, which is represented in curve a) by the peak C1 placed at -1.25V. By setting the HCl concentration in 0.01M, the predominant cathodic reaction is the reduction of iron as well, but the presence of a prepeak (C2) at about -0.5V, corresponding to hydrogen evolution, is observed. On reversing the scan, a complex anodic peak (A1) is present in the voltammograms obtained for HCl concentration values lower than 0.05M. Peak A1 is attributed to the dissolution of the different iron phases deposited during the reduction process. On the contrary, if the HCl concentration is higher than 0.05M, curve c) of Fig. 9, hydrogen evolution becomes excessive and the voltammogram main cathodic feature is the hydrogen evolution peak (C2). In the reverse anodic scan, different anodic peaks may be detected: a big peak centred at about 0V (A2) which is associated with hydrogen oxidation and peak (A'1) related to the oxidation of Fe^{2+} to Fe^{3+}. Note that the complex anodic peak (A1) is absent, because at this low pH it is virtually impossible to deposit iron [33]. The micrograph of the deposit obtained at -1.4V (not shown) for a solution composed of 0.11M $FeCl_2$ in 0.05M HCl did not show any iron crystallite, which supports the previous statement.

Fig. 10 compare the voltammetric response obtained for a zinc solution, curve a), an iron solution, curve b), and a solution containing a mixture of zinc and iron at the same concentration value as that present for the individual species, curve c).

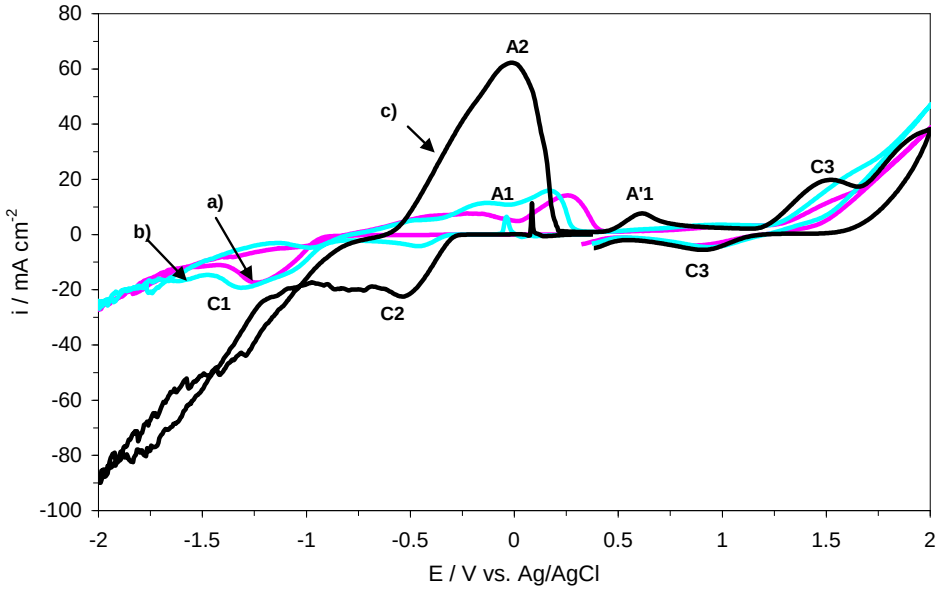

Figure 9. Cyclic voltammogram of a 0.055M $FeCl_2$ electrolyte as a function of the HCl concentration: a) 0M HCl; b) 0.01M HCl; c) 0.05M HCl. Scan rate 60 mVs^{-1}.

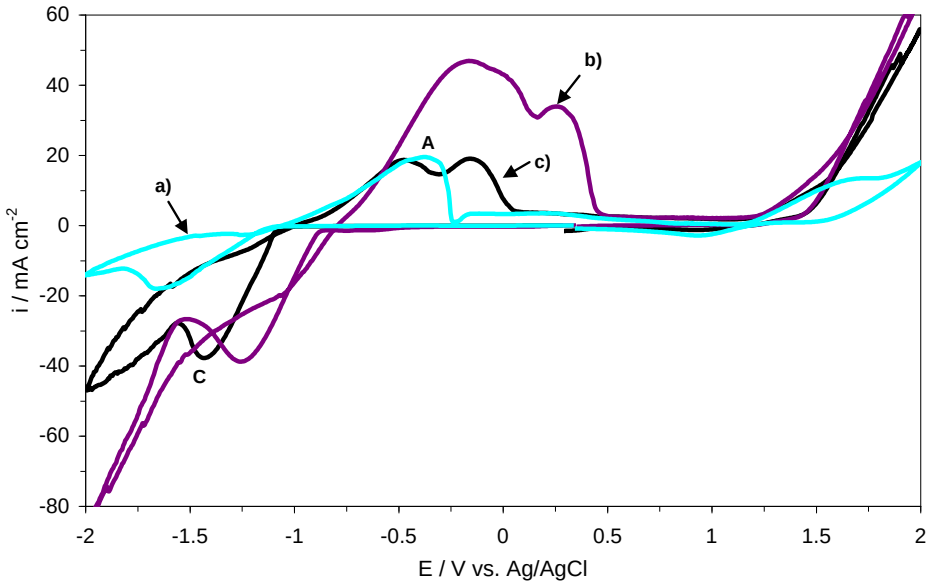

Figure 10. Cyclic voltammograms obtained for different solutions: a) 0.055M $ZnCl_2$; b) 0.11M $FeCl_2$; c) 0.11M $FeCl_2$ and 0.055M $ZnCl_2$. Scan rate 60 mVs^{-1}

The potential necessary to begin the alloy deposition is shifted to more negative values if compared to the individual iron behaviour. This suggests an inhibition of the iron deposition in the presence of zinc in solution and can be related to the electrodeposition of zinc-rich alloys [34]. A reduction peak (C) at

a potential value close to -1.5V is observed in curve c) of Fig. 10, which refers to the reduction of the zinc-iron alloy [35] and moves in the same way as the onset of the voltammetric process. In the reverse scan, a complex anodic peak (A) is present, which is attributed to the dissolution of the zinc-iron alloy, and its complex shape reveals the presence of iron in the alloy.

The ratio Fe(II)/Zn(II) in solution has a strong influence on the composition of the alloy. Fig. 11 plots the effect of the iron concentration in solution on the cyclic voltammograms, where the cyclic voltammograms of zinc, curve a), and iron, curve b), are also included to facilitate the interpretation of the data. An increase of iron in solution promotes the deposition of the alloy as shown in Fig. 11 by the displacement of the potential necessary to begin the alloy deposition towards less cathodic potentials, and by the increment of the cathodic peak of the alloy (C) and its corresponding counterpeak (A) when comparing curves c) and d). On the other hand, the increase of zinc concentration (not shown) also leads to an increase in the alloy deposition process, although the observed onset of voltammetric potential does not reach the potential corresponding to the pure-iron deposition process.

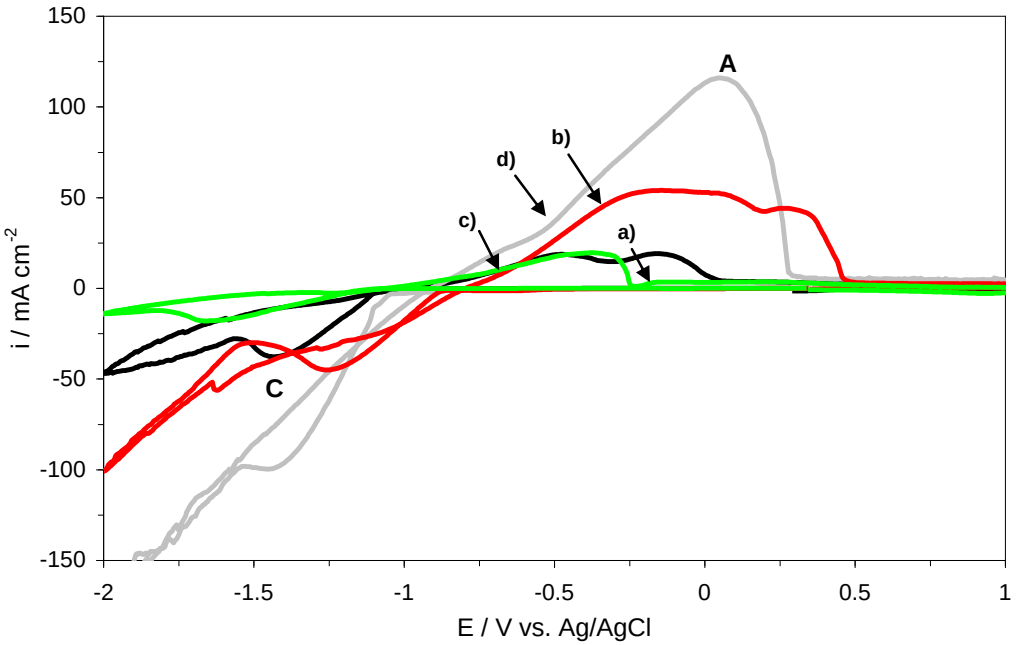

Figure 11. Cyclic voltammograms obtained for different solutions: a) 0.055M $ZnCl_2$; b) 0.125M $FeCl_2$; c) 0.11M $FeCl_2$ and 0.055M $ZnCl_2$; d) 0.495M $FeCl_2$ and 0.055M $ZnCl_2$. Scan rate 60 mVs^{-1}

For a Fe(II)/Zn(II) ratio of 2:1 in solution, curve c) of Fig. 11, the oxidation current of peak A appears at similar values to that observed for the oxidation of the zinc deposited from an iron-free solution [36]. These results are consistent with anomalous codeposition and with the inhibition of iron electrodeposition observed in the presence of zinc in solution which is related to the electrodeposition of zinc-rich alloys. The micrograph of the deposited obtained for mixtures zinc-iron in a Fe(II)/Zn(II) ratio of 2:1 and 0.1M HCl, only showed the typical morphology of the zinc deposits which confirms the anomalous deposition of zinc and the inhibition of the iron deposition at low pH.

An increase in the Fe(II)/Zn(II) ratio of 9:1, shifts the onset of the cathodic potential towards less negative values which gets closer to the onset of the cathodic curve for the pure-iron solution, curve b). This fact causes an iron enrichment of the alloy, which is also manifested by the big anodic peak (A) observed in curve d), whose potential range is similar to that obtained for the oxidation peak of the zinc-free solution, curve b).

4. CONCLUSIONS

An electrochemical study of solutions containing zinc and iron in HCl electrolyte in a concentration range similar to that found in the pickling spent baths of the galvanizing industry was carried out. Zinc deposition took place by direct formation of metallic zinc and the characteristic features of a process involving nucleation were shown in the voltammograms. Decreasing the HCl concentration enhanced the zinc UPD process because of the less influence of the hydrogen evolution reaction, in this case, a prepeak corresponding to the zinc UPD process was observed previously to the zinc OPD step. The variation of the cathodic current of the OPD peak with the scan rate showed that the bulk zinc deposition was not only controlled by diffusion but also by charge transfer kinetics. The theoretical expression for the variation of the peak current corresponding to the zinc OPD step with $\nu^{1/2}$ for an irreversible reduction process, served us to calculate the diffusion coefficient of zinc, which had a value 1.66×10^{-9} m^2s^{-1}.

An study of the influence of the inversion potential (E_λ) revealed that the anodic peak corresponding to the bulk zinc oxidation was absent when E_λ was less cathodic than -1V and under low pH. This fact was confirmed by the SEM observation of the deposits obtained at -0.5V and is a consequence of the strong influence of the hydrogen evolution reaction in the potential region more positive than -1V.

At low pH is virtually impossible to deposit iron. The electrochemical study of mixtures containing both zinc and iron showed that the presence of zinc produced an inhibition of the iron deposition process. If the ratio Fe(II)/Zn(II) was low, the shape of the voltammograms was more similar to those obtained for an iron-free solution. This fact was confirmed by the observation of the deposits obtained under these experimental conditions and at low pH values. The SEM images revealed only the presence of zinc grains. However if the ratio Fe(II)/Zn(II) was higher, the voltammograms main features were more similar to those obtained for pure iron solutions.

ACKNOWLEDGEMENT
Montserrat Garcia Gabaldón wants to express their gratitude to the Universidad Politecnica de Valencia for the economical support in the project reference: PAID-06-08, and to the Generalitat Valenciana for the financing of the project reference: GV/2010/029.

References

1. B.M. Praveen and T.V. Venkatesha, *Int. J. Electrochem. Sci.*, 4 (2009) 258
2. U. Kerney, *Resour. Conserv. Recy.*, 10 (1994) 145

3. 2C. Stocks, J. Wood and S. Guy, *Resour. Conserv. Recy.*, 44 (2005) 153
4. E. Marañón, Y. Fernández, F.J. Súarez et al., *Ind. Eng. Chem. Res.*, 39 (2000) 3370
5. A.Recéndiz, I. González and J.L. Nava, *Electrochim. Acta*, 52 (2007) 6880
6. M. García-Gabaldón, V. Pérez-Herranz, J. García-Antón et al., *J. Appl. Electrochem.*, 37 (2007) 1145
7. S. Fletcher, C.S. Halliday, D. Gates et al., *J. Electroanal. Chem.*, 159 (1983) 267
8. S. Fletcher, *Electrochim. Acta*, 28 (1983) 917
9. G. Gunawardena, G. Hills and I. Montenegro, *J. Electroanal. Chem.*, 138 (1982) 241
10. T. Casanova, F. Soto, M. Eyraud et al., *Corros. Sci.*, 39 (1997) 529
11. C. Cachet and R. Wiart, *J. Electrochem. Soc.*, 141 (1994) 131
12. K. Raeissi, A. Saatchi, M.A. Golozar et al., *Surf. Coat. Tech.*, 197 (2005) 229
13. D.J. Walton, L.D. Burke and M.M. Murphy, *Electrochim. Acta*, 41 (1996) 2747
14. L.D. Burke and K.J. O'Dwyer, *Electrochim. Acta*, 34 (1989) 1659
15. S.C. Das, P. Singh and G.T. Heftler, *J. Appl. Electrochem.*, 29 (1997) 738
16. G. Trejo, R. Ortega, Y. Meas et al., *J. Electrochem. Soc.*, 145 (1998) 4090
17. A.Gomes and M.I. da Silva Pereira, *Electrochim. Acta*, 52 (2006) 863
18. T. Boiadjieva, M. Monev, A. Tomandl et al., *J. Solid State Electrochem.*, 13 (2009) 671
19. V. Sudha and M.V. Sangaranarayanan, *J. Phys. Chem. B*, 106 (2002) 2699
20. E. Guerra, G.H. Kelsall, M. Bestetti et al., *J. Electrochem. Soc.*, 151 (2004) E1
21. A.Aramata, M.A. Quaiyyum, W.A. Balais et al., *J. Electroanal. Chem.*, 338 (1992) 367
22. M.A. Quaiyyum, A. Aramata, S. Moniwa et al., *J. Electroanal. Chem.*, 373 (1994) 61
23. P.F. Méndez, J.R. López, Y. Meas et al., *Electrochim. Acta*, 50 (2005) 2815
24. A.R. Despic and M.G. Pavlovic, *Electrochim. Acta*, 27 (1982) 1539
25. S. Taguchi, A. Aramata, M. Quaiyyum et al., *Electroanal. Chem.*, 374 (1994) 275
26. A.J. Bard and L.R. Faulkner, *Electrochemical methods. Fundamentals and Applications 2nd ed.*, John Wiley & Sons, New York (2001)
27. Z. Galus and W.A.C. Bryce, *Fundamentals of Electrochemical Analysis 2nd ed.*, Ellis Horwood, New York (1994)
28. E.R. Brown and J.R. Sandifer, *Cyclic voltammetry, AC polarography and related techniques, in B.W. Rossiter, J.F. Hamilton (Eds.). Physical Methods of Chemistry. Vol II: Electrochemical Method,*. Wiley, New York (1986)
29. M. Jayakumar, K.A. Venkatesan and T.G. Srinivasan, *Electrochim. Acta*, 53 (2008) 2794
30. U.O.S Southampton Electrochemistry Group, *Instrumental Methods in Electrochemistry*, Horwood Publishing, (2001)
31. L. Marder, E.M. Ortega-Navarro, V. Pérez-Herranz et al., *J. Membr. Sci.*, 284 (2006) 267
32. L.J. Pavlovic, M.M. Pavlovic, M.G. Pavlovic et al., *Int. J. Electrochem. Sci.*, 5 (2010) 1898
33. G. Csicsovszki, T. Kekesi and T.I. Torok, *Hydrometallurgy*, 77 (2005) 19
34. S.L. Diaz, O.R. Mattos, O.E. Barcia et al., *Electrochim. Acta*, 47 (2002) 4091
35. E. Gomez, E. Pelaez and E. Valles, *J. Electroanal. Chem.*, 469 (1999) 139
36. E. Gomez and E. Valles, *Bulletin of Electrochemistry*, 10 (1994) 477